Influence of process parameters on powder jet properties in L-DEDp using different nozzle designs

João Pedro Madeira Araujo [1,2*], *Jhonattan* Gutjahr[2], *Qingping* Yang[1], and *Diane* Mynors[1]

[1]Department of Mechanical and Aerospace Engineering, Brunel University London, Uxbridge UB8 3PH, UK
[2]TWI Technology Centre, Wallis Way, Catcliffe, Rotherham S60 5TZ, UK

Abstract. In the Laser Directed Energy Deposition (L-DEDp) process, a laser melts fine metal powder delivered through a carrier gas as a focused powder jet. The geometry and behaviour of this jet, particularly its stand-off distance and focus diameter, are directly influenced by process parameters such as carrier gas flow, shielding gas flow, and powder mass flow. These characteristics affect the interaction between the laser and the material, which influence the deposition quality. In this study, a camera-based monitoring system was employed to capture images of the powder gas jet stream (PGJS), enabling precise measurement of its geometrical features through image processing techniques. Experiments were conducted using two different nozzle designs across a wide range of process parameters to investigate how each parameter influences the jet's shape and stability. The results show that carrier gas has a dominant effect on particle velocity and jet convergence, while powder mass flow primarily impacts the jet's focus diameter. Shielding gas was found to affect stand-off distance more significantly at lower carrier gas levels. This work contributes to a better understanding of PGJS behaviour and provides valuable insights for optimising L-DEDp across different nozzle configurations.

1 Introduction

In the Laser Directed Energy Deposition process (L-DEDp) a laser is used as a thermal source to melt fine metal powder, which is fed through a nozzle as it is deposited into a metal substrate, forming a melt pool. By the relative movement between the substrate and nozzle, tracks are created to construct three-dimensional structures, coatings and repairs [1].

The nozzles used in L-DEDp are designed to guarantee a focus point between the laser beam and the powder flow [1]. Depending on the design of the nozzle, both the speed and the direction of the powder flow change, affecting the stability of the melt pool and the quality of the deposited layers [2]. Among the available nozzle arrangements, continuous coaxial and discrete coaxial nozzle types are the most used configurations. They offer considerable flexibility for material deposition regardless of the movement direction of the substrate or processing head, making them well-suited for complex geometries, despite being more complex and expensive [3].

The flow of powder is controlled via a powder feeding system [4]. When the mixture of powder and gases exit the nozzle, it creates a convergent powder jet, also called as Powder Gas Jet Stream (PGJS) [5], which creates a focal point at a certain distance of the nozzle. The geometrical characteristics of the PGJS influences where and how the powder interacts with the laser beam, with consequences on process quality and stability [6]. Figure 1 shows a schematic of the PGJS.

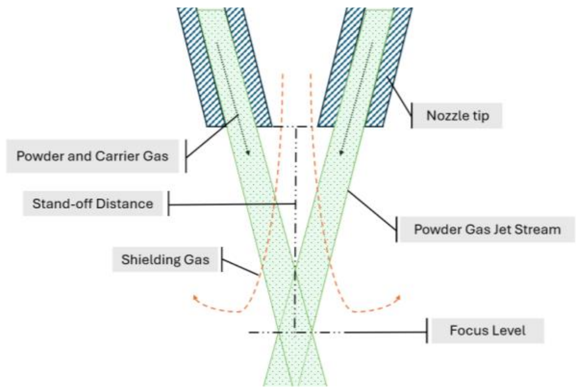

Fig. 1 Schematic of Powder Gas Jet Stream – PGJS (Author).

Some characteristics of the powder jet are estimated by the nozzle's manufacturer, e.g. the distance from the nozzle to the focus (also known as stand-off distance) and the diameter of the focus. However, variations in the powder feeding parameters, e.g. the nozzle type and geometry [7], carrier and shielding gases [8], and powder type and mass flow [9], affect the characteristics of the PGJS, changing its diameter and location, the symmetry, and the powder density along the PGJS.

To measure the PGJSs, camera-based systems can be employed [8, 10]. However, measuring is costly, due to the time and hardware involved for PGJS assessment. Benchmark data is still scarce in the available literature that quantifies the parameters' effects on the PGJS.

The aim of this work is to evaluate and quantify the influence of process parameters on the Powder Gas Jet

* Corresponding author: JoaoPedro.MadeiraAraujo@brunel.ac.uk

Stream characteristics generated by both continuous and discrete nozzle configurations. This evaluation is based on a comprehensive experimental dataset acquired through an industrial camera-based monitoring system, enabling a comparative analysis of the nozzles' performance under varied operational conditions.

2 Materials and methods

2.1 Experimental setup

All experiments were conducted at the TWI's state of the art facility for Laser-DED [11], using the Hornet Laser Cladding BV's machine platform [12]. The equipment consists of a powder conveying system, an ABB robotic arm [13], a laser beam source with optics, one rotary handling unit, one rotational workbench and a human machine interface (HMI) to regulate process parameters such as carrier and shielding gas [L/min] and powder flow rate [g/min]. The powder conveying system includes a powder feeder developed by Hornet [12] as well as a disc feeder hopper from BLC Lasercladding GmbH [14].

2.1.1 Material selection

The stainless steel 316L (8 g/cm³) was selected for the PGJS measurement. The particle size distribution (PSD) relates to the sizes and how they distribute in a range of particles. Powder focus, the distribution of particles along the powder jet, and stand-off distance are influenced by the PSD of the powder used in the process. Smaller particles are more sensitive to the carrier gas and have faster velocity, resulting in smaller and more concentrated focus diameters [17]. Larger particles, on the other hand, have lower velocities due to their inertia, affecting the powder jet's convergence and resulting in a more dispersed (or wider) powder focus [18].

For this study, a 50–90 µm stainless steel 316L powder from Metalpine [16] was used to examine how process parameters affect PGJS characteristics.

2.1.2 Nozzle selection

Coaxial nozzles inject PGJS symmetrically around the laser beam axis. Depending on how the powder is fed along the laser axis, it is classified as continuous (ring-shaped) or discrete (multi-jet) [2]. In a continuous nozzle, the powder exits through a ring-shaped cavity, creating a hollow powder jet cone that encloses the laser beam. In contrast, a discrete nozzle has multiple ejectors (or inlays) distributed around the nozzle to deliver the metal powder to the laser beam [3].

To evaluate and compare the sensitivity of the PGJS generated by continuous and discrete nozzle types, two coaxial nozzles from Harald Dickler were selected for this study. The HighNo 4.0 [19], featuring a continuous powder feed design with an annular gap of 0.4 mm, produces a focused jet with a standard stand-off distance of 9 mm and a focus diameter of 1 mm, as specified by the manufacturer (see Figure 2 - top). In contrast, the HighNo 13-6 [20] is a discrete-feed nozzle that uses six injectors arranged coaxially with the laser beam. It creates a focused PGJS with a standard stand-off distance of 13 mm and a focus diameter of 1.8 mm, using 1.5 mm injectors (see Figure 2 - bottom).

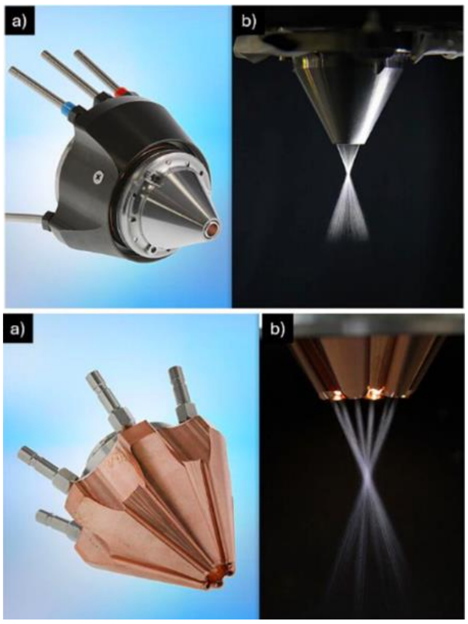

Fig. 2 Top - Coaxial continuous powder nozzle HighNo 4.0 (a) design and (b) PGJS [19]. Bottom - Coaxial discrete powder nozzle HighNo 13-6 (a) design and (b) PGJS [20].

2.1.3 Measurement system

Optical-based methods, such as digital imaging and analysis, are commercial monitoring systems used to monitor the PGJS by illuminating the particles of the powder jet with a laser light source and photographing them with a camera. It provides a non-contact method for measuring the aspects of the PGJS in multi levels by measuring layers of illuminated particles [21].

Two main camera setups are typically used in these measurement systems: coaxial [10] and lateral (or off-axis) [7]. The key difference lies in how the camera is positioned in relation to the powder jet. Each configuration comes with its own advantages and limitations when it comes to cost, flexibility, and usability.

Cameras capable of capturing up to 100 frames per second are commonly used in both setups to record images of the PGJS [10]. To avoid motion blur from the fast-moving particles, the camera's exposure time is carefully adjusted [22]. These images are usually taken in grayscale, where each pixel reflects light intensity on a scale from 0 (dark) to 255 (bright) [2]. Once the images are captured, background subtraction helps remove fixed elements like the nozzle, making the powder particles stand out more clearly [13]. After that, the images go through a thresholding process that turns them into black-and-white (binary) versions, which helps isolate individual particles for further analysis [10]. Choosing an appropriate threshold value is essential for accurately detecting particles and calculating the focus diameter of the jet.

Beyond identifying particles, image intensity is analysed to estimate particle concentration within the stream [8]. Higher reflected intensity indicates a denser powder flow, and this data can be visualised through heatmaps or "powder caustics," which show how the jet converges into a focused stream [9, 22, 23]. Studies have shown that a Gaussian distribution effectively models the intensity profile of PGJSs [8-10, 23], allowing the determination of key metrics like stand-off distance and focus diameter [8].

In this study, the LIsec® system developed by Fraunhofer IWS [24] was selected. It uses a vertical illumination laser (50 µm line width, 785 nm wavelength) to light up the powder particles, which are captured by a camera with 34.54 µm resolution. The captured images are processed using the PowderNozzle 2.13 software [24], which analyses the pixel intensity to generate horizontal and vertical intensity profiles of the PGJS.

These profiles offer insights into the jet's behaviour: the horizontal profile slices the jet to show particle distribution across its width, allowing focus diameter measurement at the point of highest concentration. Meanwhile, the vertical profile examines the intensity distribution along the Z-axis to determine the stand-off distance, defined as the gap between the nozzle tip and the jet's focal point, by tracking where the particles converge from a lateral view.

2.2 Design of experiment

The experimental design follows a full factorial approach. By covering a larger set of parameters, it is possible to examine the influence of each factor in the behaviour of the PGJS, providing deeper details of the tendencies.

The objective of the test is to evaluate the influence of gases and powder mass flow (PMF) rate on the PGJS across both nozzle designs by testing on the measurement devices. The range of carrier gas (CG) levels used for this experiment follows common values discussed in the literature and in industrial applications [51], between 3 L/min and 9 L/min (factor of 3 L/min). Furthermore, the range of shielding gas (SG) evaluated starts at 0 L/min, used as a baseline, and 5 L/min to 15 L/min, as the range explored by Bohlen [7]. The PMF was 10, 20, and 30 g/min [22], using SS 316L powder with a PSD of 50-90 µm. Gas flow settings are checked with a mass flow sensor from ALICAT [25] to confirm they match the software's input values, and the powder feed rate is measured twice using a Sartorius precision scale [26] to ensure accuracy.

3 Results and discussions

3.1 Random and systematic error

To ensure the reliability of the measurements, a selected test condition was repeated in the beginning, midway and again at the conclusion of the experiments. The variation observed between these repeated measurements is used to estimate the random error associated with the dataset. Additionally, systematic error is determined by comparing the actual dimension of a reference object with the corresponding measurement obtained from the image processing software. The results are presented in Table 1.

Table 1. Random and Systematic error of the measurements

Nozzle	Parameter Output	Random Error (%)	Systematic Error (%)
HighNo 4.0	Stand-off Distance	0.92	0.25
	Focus Diameter	8.17	
HighNo 13-6	Stand-off Distance	0.53	
	Focus Diameter	1.41	

The calculated measurement uncertainties, with both random and systematic errors kept to a minimum, indicate a high degree of consistency and reliability in the experimental setup. For both nozzles tested (HighNo 4.0 and HighNo 13-6), the random error observed in the stand-off distance remains well below 1%, while for focus diameter it keeps below 10%. These values suggest a relatively stable and repeatable measurement process, especially considering the complexity of the PGJS dynamics.

The systematic error found for the measurement system is small, reinforcing the precision of the measuring system. Considering the low level of both errors, it supports the validity of the data and confirms that the observed trends are statistically representative. The following sections present and discuss the key findings from this analysis.

3.2 Continuous nozzle (HighNo 4.0)

By analysing the data collected through the experiments, it is possible to observe the strong influence of the shielding gas on the stand-off distance. Increasing the shielding gas flow rate induces a downshift of the PGJS's focal plane in this nozzle configuration. This behaviour can be visualised in Figure 3.

The carrier gas, on the other hand, exhibits inverse influence on the stand-off distance, suggesting that as carrier gas levels increase, the intersection of the powder jet happens closer to the nozzle exit. Interestingly, the variance in stand-off distance is stronger at lower carrier gas flow rates, implying that slower particle movement on the PGJS results in greater variation in particle convergence area. The powder mass flow did not influence much the stand-off distance values, affecting more the PGJS's focus diameter as shown in Figure 4.

It is possible to observe in Figure 4 a clear trend: as the PMF increases, so does the focus diameter. This relationship is most apparent at lower carrier gas flow rates, as illustrated by the box plots. For instance, at a carrier gas flow of 3 L/min, the median focus diameter increases with PMF, and the interquartile range becomes wider, particularly for the highest PMF (30 g/min), indicating greater variability and a more dispersed powder jet when the particles are travelling slower within the PGJS. The outliers presented at this condition suggest an inconsistent jet behaviour.

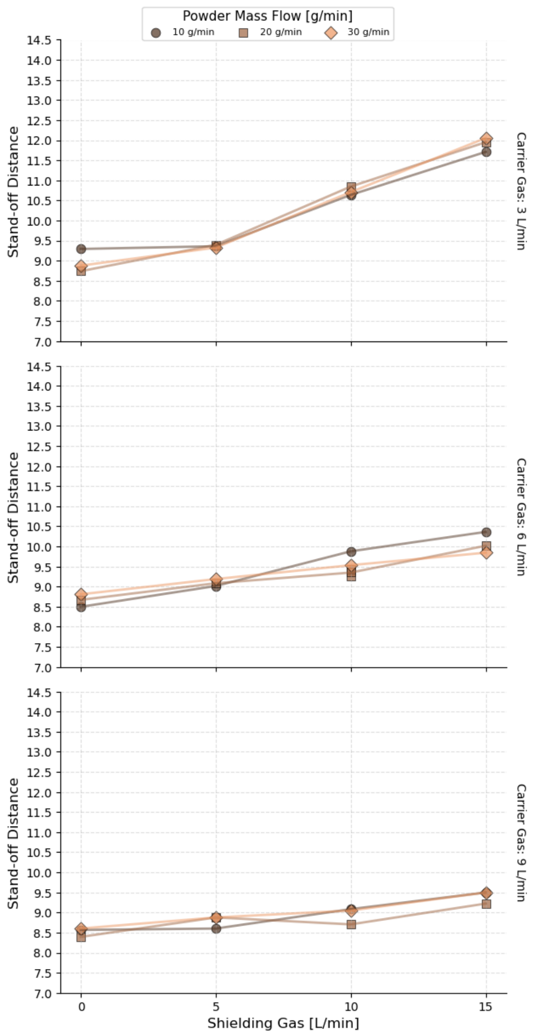

Fig. 3 Line plots of Stand-off distance values of HighNo 4.0 for levels of shielding gas, separated by carrier gas and powder mass flow rate (Author).

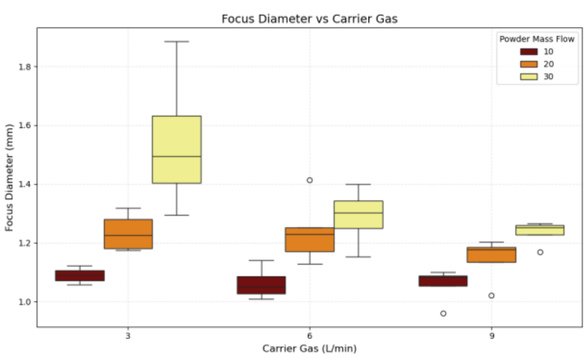

Fig. 4 Box plot of carrier gas and powder mass flow influence on focus diameter of HighNo 4.0 (Author).

In contrast, as the carrier gas flow increases to 6 and 9 L/min, the box plots show a narrowing of the interquartile range and a downward shift in the median focus diameter for all levels of powder mass flow. This suggests that increased carrier gas rates induce a more concentrated and stable jet, which decreases PMF's influence and spread. At a carrier gas flow of 9 L/min, the box plots show a clear narrowing across all PMF levels, suggesting that the influence PMF is significantly reduced under these conditions. This noticeable decrease in data spread with fewer outliers, like what was observed for stand-off distance, indicates that higher carrier gas flow contributes to a more stable and consistent jet. These patterns lend strong support to the idea that the carrier gas plays a dual role: not only does it enhance particle velocity, but it also actively shapes the behaviour of the PGJS, particularly in conditions where lower flow rates would likely introduce more fluctuation.

3.3 Discrete nozzle (HighNo 13-6)

The variability in stand-off distance and focus diameter of the HighNo 13-6 nozzle follows a different pattern when compared with the HighNo 4.0. The stand-off distance is relatively stable, with minor fluctuations depending on the CG and SG conditions. For the continuous nozzle, the stand-off distance ranges from approximately 8.4 mm to 12 mm, presenting some outliers with changes largely occurring in response to variations in shielding gas flow and carrier gas flow. In discrete configuration, the stand-off is less sensitive to the input parameters, ranging from 12.05 mm to 12.74 mm, with no outliers during the variation of the flow rate, as presented in Figure 5.

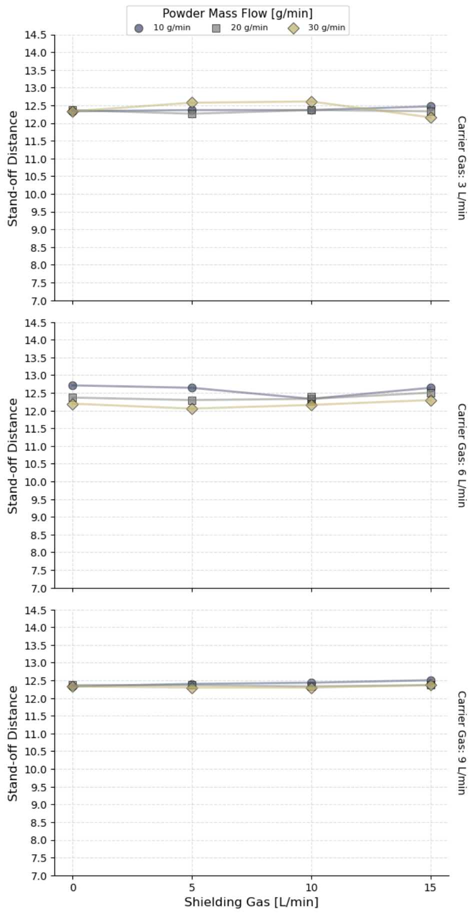

Fig. 5 Line plots of Stand-off distance values of HighNo 13-6 for levels of shielding gas, separated by carrier gas and powder mass flow rate (Author).

Changes in powder mass flow also do not have a pronounced effect on the stand-off distance, showing higher influence on the focus diameter, as illustrated in Figure 6.

The box plot reveals a clear trend in how the focus diameter responds to changes in PMF. By increasing the amount of powder delivered in the process, the focal diameter tends to increase as well as reducing the variance in higher powder mass flows. It can be confirmed by observing the small increment in the median, indicating that wider focus is generated by delivering more particles into the jet.

In addition, the variability of the focal diameter on the discrete configuration, around 0.35mm, is smaller when compared to HighNo 4.0, where the focus varies around 1mm. This can be related to the design of discrete nozzles. The insertion of particles through isolated inserts seems to be less influenced by the combination of powder jets, whereas continuous nozzles, the mixture of gases and particles, have a greater effect on particle distribution and trajectory within the annular gap exit.

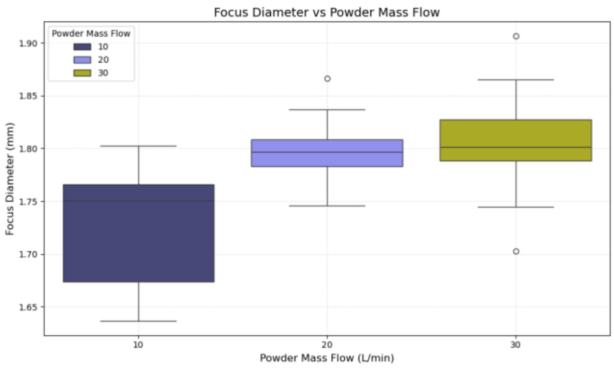

Fig. 6 Box plot of powder mass flow influence on focus diameter of HighNo 13-6 (Author).

4 Conclusion

In conclusion, the data collected with the LIsec® measurement systems for the continuous (HighNo 4.0) and discrete (HighNo 13-6) coaxial powder nozzles, highlights the impact of process parameters such as shielding gas, carrier gas and powder mass flow rate on the PGJS's stand-off distance and focus diameter.

While both nozzles follow similar trends, the influence of the parameters is more pronounced on continuous nozzle design. For both nozzles, the correlation between shielding gas and focus diameter is positive: the higher the SG flow, the larger is the focal diameter. Similarly, the shielding gas has a positive correlation with the stand-off distance, with larger influence on the HighNo 4.0. The HighNo 13-6 demonstrates a steadier behaviour throughout the variety of parameters.

Furthermore, carrier gas also has a pronounced impact on the variation of the stand-off distance and focus diameter for both nozzles, although with a negative correlation. As the level of gas increases, the particle's velocity rise, projecting straighter trajectories after nozzle's output, which results in the convergence of the jets closer to the nozzles and enhanced concentration (smaller size). The HighNo 4.0 nozzle is more sensitive to variations of the carrier gas, more evident at higher powder mass flows, whereas the HighNo 13-6 nozzle is less influenced by this effect.

These findings show that, while the fundamental relationships between gas flows and powder mass flow remain consistent, the distinct operating principles of each nozzle, continuous and discrete, have a significant impact on their respective responses to these variables.

Future work will focus on the application of AI and machine learning techniques to model the complex interactions between process parameters and powder jet characteristics. By leveraging machine learning algorithms, it will be possible to predict jet behaviour and optimise process settings more efficiently. The outcomes of this ongoing research will be reported in future publications.

References

1. A. Guner, P. Bidare, A. Jiménez, S. Dimov, and K. Essa, 'Nozzle Designs in Powder-Based Direct Laser Deposition: A Review', Sep. 01, 2022, *SpringerOpen*. doi: 10.1007/s12541-022-00688-1.
2. S. P. Kumar, S. Elangovan, R. Mohanraj, and B. Srihari, 'Critical review of off-axial nozzle and coaxial nozzle for powder metal deposition', *Mater Today Proc*, vol. 46, no. 3, pp. 8066–8079, 2021, doi: 10.1016/j.matpr.2021.03.037.
3. J. Gutjahr, 'Método para reutilização de pó de aço inoxidável 316L processado por deposição de laser de energia direcionada', PhD Dissertation, Universidade Federal de Santa Catarina, Florianópolis, 2022.
4. A. J. Pinkerton and L. Lin, 'Modelling powder concentration distribution from a coaxial deposition nozzle for laser-based rapid tooling', *J Manuf Sci Eng*, vol. 126, no. 1, pp. 33–41, 2004, doi: 10.1115/1.1643748.
5. J. Gutjahr, M. Pereira, J. M. Sá de Sousa, H. S. Ferreira, and A. T. Júnior, 'Powder degradation as a consequence of laser interaction: A study of SS 316L powder reuse on the laser directed energy deposition process', *J Laser Appl*, vol. 36, no. 1, Feb. 2024, doi: 10.2351/7.0001093.
6. T. Schopphoven, N. Pirch, S. Mann, R. Poprawe, C. L. Häfner, and J. H. Schleifenbaum, 'Statistical/numerical model of the powder-gas jet for extreme high-speed laser material deposition', *Coatings*, vol. 10, no. 4, Apr. 2020, doi: 10.3390/coatings10040416.
7. A. Bohlen, T. Seefeld, A. Haghshenas, and R. Groll, 'Characterization of the powder stream propagation behavior of a discrete coaxial nozzle for laser metal deposition',

J Laser Appl, vol. 34, no. 4, Nov. 2022, doi: 10.2351/7.0000775.

8. Z. Jardon, P. Guillaume, J. Ertveldt, M. Hinderdael, and G. Arroud, ‘Offline powder-gas nozzle jet characterization for coaxial laser-based Directed Energy Deposition’, *Procedia CIRP*, vol. 94, no. 94, pp. 281–287, Sep. 2020, doi: 10.1016/j.procir.2020.09.053.
9. T. Baily, ‘In-situ Monitoring of Powder Flow in Directed Energy Deposition Additive Manufacturing’, Master Thesis, The Pennsylvania State University, Pennsylvania, 2021.
10. L. de Melo, ‘Powder jet particle density distribution analysis and qualification for the laser metal deposition process’, Master Thesis, Universidade Federal de Santa Catarina, Florianópolis, 2015. Accessed: Jan. 18, 2025. [Online]. Available: https://api.semanticscholar.org/CorpusID:136054752
11. TWI Limited, ‘Additive Manufacturing’, Wallis Way, Catcliffe, Rotherham. Accessed: Feb. 11, 2025. [Online]. Available: https://www.twi-global.com/what-we-do/research-and-technology/technologies/additive-manufacturing
12. Hornet Laser Cladding. Accessed: Feb. 18, 2025. [Online]. Available: https://www.hornetlasercladding.com/
13. ABB Ltd. Accessed: Feb. 18, 2025. [Online]. Available: https://new.abb.com/products/robotics
14. BLC Lasercladding GmbH, ‘BLC Powder Hopper’. Accessed: Feb. 18, 2025. [Online]. Available: https://blc-lasercladding.de/PRODUKTELEISTUNGEN/ERSATZTEILE-ZUBEHOeR
15. R. Groarke, C. Danilenkoff, S. Karam, E. McCarthy, B. Michel, A. Mussato, J. Sloane, A. O’Neill, R. Raghavendra, D. Brabazon ‘316l stainless steel powders for additive manufacturing: Relationships of powder rheology, size, size distribution to part properties’, *Materials*, vol. 13, no. 23, pp. 1–19, Dec. 2020, doi: 10.3390/ma13235537.
16. Metalpine, ‘Metalpine spherical powder data sheet’, 2023. Accessed: Feb. 17, 2025. [Online]. Available: https://metalpine.at/blog/news-updates-1/post/316l-metalpine-powder-as-quality-benchmark-27
17. L. Li, Y. Huang, C. Zou, and W. Tao, ‘Numerical study on powder stream characteristics of coaxial laser metal deposition nozzle’, *Crystals (Basel)*, vol. 11, no. 3, Mar. 2021, doi: 10.3390/cryst11030282.
18. X. Gao, X. X. Yao, F. Y. Niu, and Z. Zhang, ‘The influence of nozzle geometry on powder flow behaviors in directed energy deposition additive manufacturing’, *Advanced Powder Technology*, vol. 33, no. 3, Mar. 2022, doi: 10.1016/j.apt.2022.103487.
19. Harald Dickler, ‘HighNo 4.0’. Accessed: Feb. 08, 2025. [Online]. Available: https://hd-sonderoptiken.de/fileadmin/documents/Produktblatt_-_HighNo_4.0.pdf
20. Harald Dickler, ‘HighNo 13-6’. Accessed: Feb. 08, 2025. [Online]. Available: https://hd-sonderoptiken.de/fileadmin/files/Products/documents/Produktblatt_-_HighNo_13_-_6.pdf
21. S. Zekovic, R. Dwivedi, and R. Kovacevic, ‘Numerical simulation and experimental investigation of gas-powder flow from radially symmetrical nozzles in laser-based direct metal deposition’, *Int J Mach Tools Manuf*, vol. 47, no. 1, pp. 112–123, Jan. 2007, doi: 10.1016/j.ijmachtools.2006.02.004.
22. E. Ferreira, M. Dal, C. Colin, G. Marion, C. Gorny, D. Courapied, J. Guy, P. Peyre, ‘Experimental and numerical analysis of gas/powder flow for different LMD nozzles’, *Metals (Basel)*, vol. 10, no. 5, May 2020, doi: 10.3390/met10050667.
23. Z. Liu, H. C. Zhang, S. Peng, H. Kim, D. Du, and W. Cong, ‘Analytical modeling and experimental validation of powder stream distribution during direct energy deposition’, *Addit Manuf*, vol. 30, Dec. 2019, doi: 10.1016/j.addma.2019.100848.
24. Fraunhofer Institute for Material and Beam Technology IWS, ‘LIsec-Nozzle Measuring System Instruction Manual’, Jul. 30, 2024. Accessed: Apr. 03, 2025. [Online]. Available: https://www.iws.fraunhofer.de/content/dam/iws/en/documents/publications/product-sheets/2024_Product-Sheet_LIsec_EN.pdf
25. ALICAT Scientific, ‘STANDARD FLOW AND PRESSURE DEVICES’, Apr. 2024. Accessed: Apr. 03, 2025. [Online]. Available: https://documents.alicat.com/manuals/DOC-MANUAL-MPL.pdf
26. Sartorius, ‘Quintix® Pro’, 2023. Accessed: Feb. 25, 2025. [Online]. Available: https://www.sartorius.com/download/1518854/analytical-balance-lab-weighing-quintix-pro-datasheet-en-sar-1--data.pdf